

STM study of gold-overlayer formation on C_{60} monolayers

Zhao Y. Rong

*Physics Department, Brookhaven National Laboratory, Upton, New York 11973
and Physics Department, State University of New York–Stony Brook, Stony Brook, New York 11794*

L. Rokhinson

*Physics Department, State University of New York–Stony Brook, Stony Brook, New York 11794
(Received 10 November 1993)*

Scanning tunneling microscopy was used to study Au-overlayer formation on the first and second monolayers of C_{60} on a Au(111) substrate. At 300 K, Au overlayers were clustering on top of the first monolayer of C_{60} , and the stronger Au-Au bonding did not break the underlying long-range close-packed order of C_{60} molecules. However, Au diffused under the second C_{60} layer and formed two-dimensional clusters. These clusters provided multiple nucleation sites and the second C_{60} monolayer was rearranged around them. As a result, the second monolayer granulated. Bonding between the second monolayer and underlying Au clusters, characterized by charge transfer, was evidence that density of states near the Fermi level became higher. Our real-space images clarified some details presented in a recent photoelectron spectroscopy study.

INTRODUCTION

Since the breakthrough of fullerene synthesis,¹ many applications have been proposed. Among them is fullerene thin-film coating. C_{60} thin films have been studied extensively by scanning tunneling microscopy (STM) and other means.² It has been found that the first monolayer bonds strongly with many substrates, including Au, for which no carbide is expected. The second monolayer, however, is relatively mobile at 300 K. An important issue toward applications of C_{60} thin films in nanotechnology is the preparation of metal contacts. In a recent photoelectron spectroscopy study by Ohno *et al.*,³ it was found that Au overlayers were clustering on C_{60} thin films. It has also been speculated that this clustering may lead to roughening of the starting surface, which may provide a guide in understanding the nature of Au- C_{60} interface.

We report scanning tunneling microscopy results for Au overlayer formation on the first and second monolayers of C_{60} on a Au(111) substrate. Combined with previously published STM and photoelectron spectroscopy results, our observations enable us to derive a comprehensive picture of diffusion, nucleation, and modification at the Au- C_{60} interface.

EXPERIMENT

The STM used in this study is a homemade unit based on an electrical remote control scheme of tip approach, similar to the design by Pan *et al.*⁴ Figure 1 is a schematic drawing of the STM head. The sample was spring clamped against a rigid STM body made of Macor. A piezoelectric tube scanner was glued onto a quartz rod which was clamped by a Teflon coated spring wire against four shear-piezo plates. The four plates were glued onto a 60° cutoff in the Macor body. An important modification to the conventional “slip-stick” tip ap-

proach,⁵ is that at the “slip phase,” the shear-piezo plates were driven one by one instead of together, therefore only one piezo plate slipped against the quartz rod at a time, while the other three plates (rather than inertial force) held the rod in position. After the completion of four “slip” steps, the four piezo plates were driven together in the opposite direction (the “stick phase”), and they carried the rod together with them. This scheme makes possible more rigid clamping, reducing vibrational noise during experiments. The STM control unit was purchased from RHK (Model STM100), with an additional high-voltage board to provide a total of four pairs of high-voltage outputs (± 130 V) for driving the shear-piezo plates.

STM images in this experiment were taken in the constant current mode with tunneling current set at around 1 nA. Tip-sample bias voltages were set around 130 mV, with the tip positive with respect to the sample. STM tips were cut from PtIr (80%/20%) wire. Imaging was carried out in air at room temperature. All images presented in this paper were original data without data

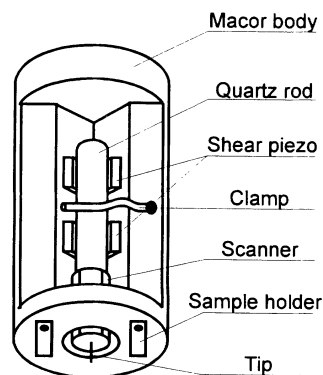


FIG. 1. Schematic diagram of the STM unit.

processing, except a plane correction to remove the sample tilt.

To obtain Au films with large flat regions, we followed a procedure similar to that described by DeRose *et al.*⁶ Three freshly cleaved mica substrates were mounted on a copper base and baked at 440°C in vacuum for 18 h before film evaporation. During this time pressure in the evaporation chamber was 3×10^{-7} torr. 1500 Å of gold (99.99%) was evaporated at the rate of 1.5 Å/s. The pressure rise during evaporation did not exceed 8×10^{-7} torr, and the sample temperature was kept at 440°C. After annealing at the same temperature for 1 h, samples were slowly cooled down to room temperature over 2 h. Film thicknesses were measured by a quartz thickness monitor. Sample No. 1 was then protected by a shutter from further evaporation. 1.7 monolayer (ML) C₆₀ was deposited on the remaining two Au films using a commercial C₆₀/C₇₀ 8:1 mixture which was sublimed in vacuum from a Ta effusion source. This source was a Ta foil tube about $\frac{1}{8}$ in. in diameter filled with C₆₀, with several pin holes punched in one side. The source was equipped with a K-type thermocouple and the temperature (500°C) was closely monitored during C₆₀ deposition to ensure the selective evaporation of pure C₆₀. Sample No. 2 was then also protected by the shutter. We then vapor deposited 2–3-Å Au on the remaining sample (sample No. 3) with an evaporation rate of 0.1 Å/s. After the samples were removed from the vacuum chamber, they were stored in a dessicator. Their STM images were taken one by one within 48 h.

RESULTS AND DISCUSSION

Our STM images on Au film (sample No. 1) show that the film is characterized by large atomic flat terraces (~ 1000 Å), similar to images presented in Ref. 6. Au grows epitaxially in the (111) direction on mica at an evaluated substrate temperature.⁷ Focusing on the top of these terraces, we can see a hexagonal close-packed structure with interatomic distances 2.9 Å and z corrugation 0.13 Å, the diagnostic of an unreconstructed Au(111) surface (Fig. 2).

STM images of sample No. 2 show that 1.7-ML coverage of C₆₀ did not change the micrometer scale morphology of the underlying Au film, as one might expect. However, detailed images on these 1000-Å-size terraces show a typical flat-hole structure (Fig. 3). The image shows a circular hole which has a depth of about 7 Å, slightly less than an expected value of 8.1 Å for a (111) step on bulk fcc C₆₀.⁸ Ordered close-packed arrays of intermolecular spacing of 11 Å and a z corrugation of 0.8 Å (Fig. 4) can be observed on the flat region inside the hole with the tip bias at +134 mV, well below the highest occupied molecular orbital–lowest unoccupied molecular orbital (HOMO-LUMO) gap voltage of bulk C₆₀ of 1.6 V.⁹ The same structure and intermolecular spacing has been reported for a monolayer of C₆₀ on a Au(111) substrate.² The possibility of imaging a C₆₀ monolayer with low bias voltage indicates the existence of states near the Fermi level. These are LUMO- or HOMO-derived states due to the charge transfer from the Au substrate.¹⁰ On

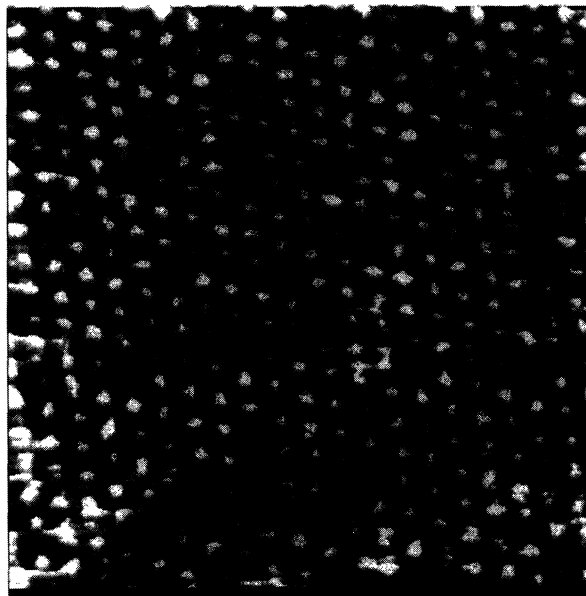


FIG. 2. Image (61×64 Å) on a flat terrace of sample No. 1 (1000-Å Au on mica). Tip bias voltage was +10 mV. The z corrugation is 0.13 Å.

the flat region outside the circle, STM images with the same tip bias were much noisier than those inside. The second monolayer of C₆₀ on Au(111) is expected to be insulating as in the bulk crystal. High quality STM images of the second monolayer of C₆₀ were observed by Altman and Colton in an UHV system with a tip bias between 2.5 and 3.0 V; that is above the HOMO-LUMO gap.² The increase of tip bias in our case, with STM operated in air, also raises the noise level (probably because there is a



FIG. 3. Image (1004×1006 Å) of C₆₀ thin film of 1.7 ML on Au(111) (sample No. 2). Area inside the circular hole is identified as the first layer of C₆₀, while the outside is the second C₆₀ monolayer. The layer spacing is 7 Å.

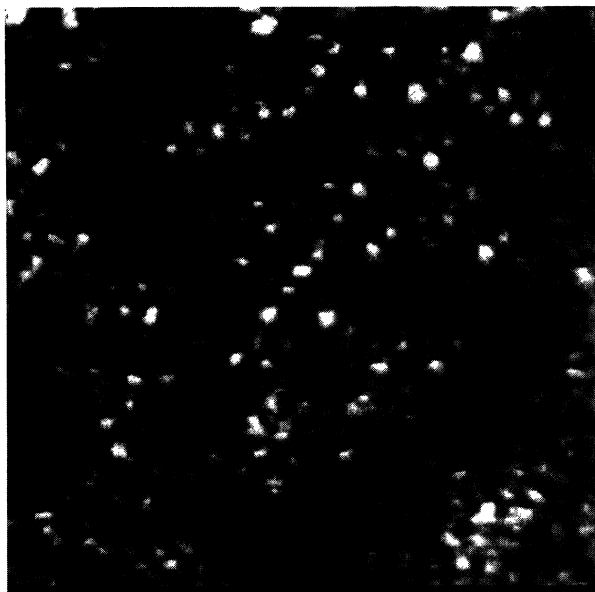


FIG. 4. Image ($230 \times 230 \text{ \AA}$) of the region inside the round hole in Fig. 3. The ordered close-packed lattice of C_{60} is shown. Periodicity is 11 \AA . Average corrugation is 0.8 \AA .

contamination layer on the sample). However, an ordered hexagonal lattice (Fig. 5) can still be imaged on our sample with a low tip bias of $+134 \text{ mV}$, and it shows a surprisingly large z corrugation of about 2 \AA , compared to Fig. 4. Enhanced z corrugations were commonly observed on samples whose transport properties are dominated by the π orbitals, e.g., graphite. A mechanism was proposed by Soler *et al.* by which the enhancement is induced by tip-sample interaction.¹¹ The same arguments can also apply here, that the lower density of states of π

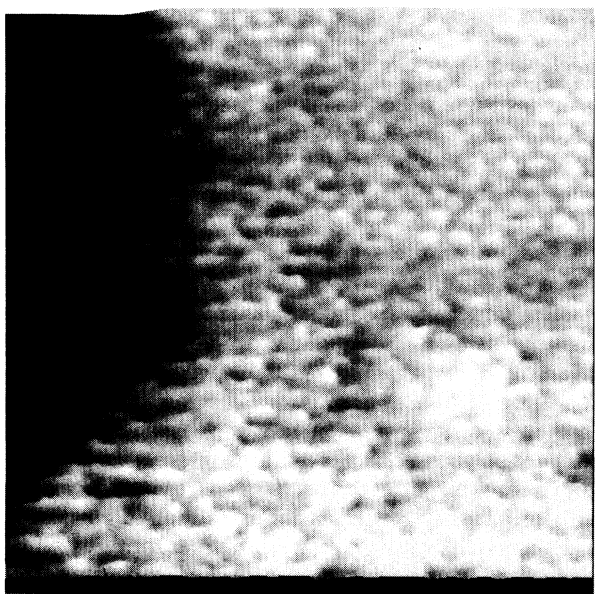


FIG. 5. Image ($214 \times 214 \text{ \AA}$) of the region at the right edge of the round hole in Fig. 3. The ordered close-packed structure is visible at the upper-right corner with a z corrugation of 2 \AA .

electrons near the Fermi level, and therefore the stronger tip-sample interaction, causes the observed larger z corrugation for the second C_{60} layer. The ratio of relative areas of high and low plateaus estimated from larger scans is close to that expected based on the 1.7-ML coverage of C_{60} indicated by the quartz thickness monitor. C_{60} molecules of the second monolayer are sufficiently mobile to form a thermodynamically favorable shape. At low coverage (1.25 ML) they form round islands,² and at high coverage (1.7 ML) they form circular holes as shown in Fig. 3. Therefore, it can be clearly identified that the lower region inside the hole in Fig. 3 is the first C_{60} monolayer which is in direct contact with Au(111) substrate, while the higher flat region outside the hole is the second C_{60} monolayer. Both of them were well-ordered close-packed fcc layers, though the second layer was much more difficult to image in the air.

Figure 6 is a $1500 \times 1500\text{-\AA}$ scan of sample No. 3, after vapor deposition of an additional 2-\AA Au on a substrate similar to sample No. 2, where terraces with flat-hole structure can still be recognized compared to Fig. 4. However, although the region inside the holes (the first C_{60} monolayer) remained flat, the surrounding higher region (the second C_{60} monolayer) changed to a granular structure. On the flat region inside the hole, bright clusters can be imaged on top of the undisturbed C_{60} hexagonal lattice with nearly the same z corrugation as in Fig. 3. Figure 7 is an example with a cluster size of 80 \AA and an apparent height of 8 \AA . The cluster was stable for at least 20 scans. The atomic (or molecular) structure was not resolved on top of the cluster; however, I - V spectroscopy at room temperature on the cluster shows metallic behavior, indicating a Au cluster. Outside the hole the

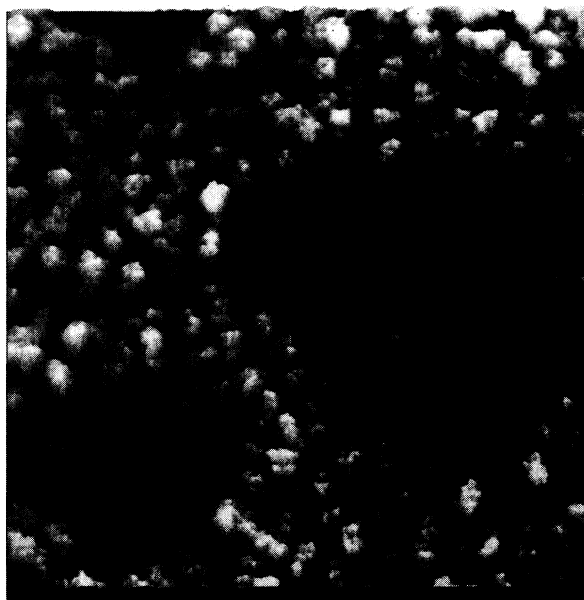


FIG. 6. Image ($1503 \times 1503 \text{ \AA}$) of sample No. 3 with 2 \AA of Au overlayers on top of a C_{60} thin film (similar to sample No. 2). It shows that a lower round region is flat and the higher region is granular. The granular region is 8 \AA higher than the flat region. The average z corrugation between grains is 3 \AA . The average grain-grain distance is 90 \AA .

original flat surface is replaced by a granular structure with the average grain-grain distance of 90 Å and a z corrugation of 3 Å. A closer look (Fig. 8) shows that these are C_{60} grains with local close-packed order and an average 0.8-Å molecular z corrugation. Molecular resolved images were much easier to obtain compared to those on the second monolayer of sample No. 2 (Fig. 5). Clusters other than C_{60} molecules were not identified within each grain. A few large clusters similar to that in Fig. 7 also can be found on top of these C_{60} grains.

In a recent photoelectron spectroscopy study by Ohno *et al.*,³ it was concluded from the slow attenuation of C 1s emission and the unchanged characteristics of Au 4f_{7/2} core level with increasing Au coverage, that Au atoms were clustering on C_{60} thin films. Our STM observation (Fig. 7) shows that large three-dimensional (3D) clusters, probably after coalescence at 300 K from smaller clusters, sit on top of the first C_{60} monolayer. It is very similar to STM images of Au overlayers on graphite (0001) surface in an air ambient condition. The fact that a z corrugation with a tip bias of +130 mV is the same before and after Au overlayer deposition also supports Au clustering rather than coating of a thin layer. Some of the deposited Au atoms can possibly diffuse under the C_{60} layer to occupy available octahedral sites between the $C_{60}(111)$ layer and the flat Au surface. However, clustering occurs only on the top since the C_{60} monolayer is not disturbed. This indicates that even strong Au-Au bonding is not enough to distort the rigid C_{60} close-packing structure on a Au(111) surface. The stability of the C_{60} monolayer on Au(111) has been characterized by a high melting temperature (600 °C) and the lifting of the underlying Au(111) ($\sqrt{3} \times 22$) reconstruction.² It has been found that a single C_{60} molecule is mobile on the Au(111) surface at 300 K, while aggregates containing two or



FIG. 7. Image (303×303 Å) inside the flat region in Fig. 6. The bright hill is around 80 Å in diameter and 8 Å in height. The underlying ordered structure is the same as in Fig. 4, with a z corrugation of about 0.8 Å.



FIG. 8. Image (152×152 Å) of a single grain on the higher region in Fig. 6. Images of the locally ordered C_{60} lattice are much easier to obtain than in Fig. 5. The average z corrugation is 0.8 Å.

more molecules are not mobile.² Our observation of Au clustering only on top of the C_{60} monolayer further confirms the strength of the close-packed structure. For future studies, it will be interesting to increase the reactivity of overlayer material, e.g., Ag, Cr, or In, to see when long-range close-packed order begins to break.

Our STM images show that the second C_{60} layer on the Au(111) substrate is roughened by Au overlayers. Photoelectron spectroscopy study³ suggests that the roughening is mediated by cluster rather than atom reaction. We did not observe Au cluster associated with each of the C_{60} grains. Molecular corrugation on these grains matches the corrugation on the first layer, which, again, indicates there is no Au layer coating on these grains. In a recent study by Sarkar and Halas,¹² the diffusion of Ag atoms into C_{60} films was observed through an electrical conductivity measurement. Therefore, it is very plausible that Au atoms, following the same process as that of Ag, diffused under the second C_{60} layer. z corrugation between C_{60} grains is only 3 Å, which suggests that Au clusters under the second C_{60} layer are very flat, probably two dimensional. A similar example is that an Au overlayer on clean graphite (0001) surface under an UHV condition forms 2D islands.¹³ Therefore we would expect that cluster formation on top of the exposed first layer and under the second layer are different. Average distance between C_{60} grains (90 Å) is therefore associated with the density of nucleation sites for Au clustering. It is determined by the substrate temperature, evaporation speed, and Au- C_{60} interaction. The nearly uniform C_{60} grain size and random arrangement can be explained by the surface diffusion dynamics. Previously mobile C_{60} molecules of the second layer rearranged their position due to the stronger Au- C_{60} bonding, toward the nearest

Au cluster. This is consistent with the facilitation of STM imaging of the second layer at low bias voltages. Direct contact with Au clusters introduced states near the Fermi level for the second C₆₀ monolayer, as it did for the first one. An STM image of an evaporated C₆₀ monolayer on a polycrystalline Au substrate has been reported to be granular,¹⁴ very similar to our modified second monolayer. Larger 3D clusters were also found on top of the granular second layer, suggesting the completion of bonding of the second layer with Au clusters.

Our data confirm the result of photoemission experiment³ that Au forms clusters on C₆₀ films. From our STM images, we can also conclude that (1) Au atoms diffuse through loose C₆₀ layers; (2) Au clusters bond to C₆₀ molecules; and (3) Au atoms do not diffuse through a C₆₀ layer which has bonded to Au clusters, and this eventually blocks the bulk diffusion. Therefore, the formation of Au overlayers on a C₆₀ film depends on the interplay between diffusion, clustering, and cluster-C₆₀ bonding. The bulk diffusion also explains why the attenuation and shifting (toward a chemisorbed C₆₀ line shape) of C 1s emission were slow with increasing Au coverage.³ A clearer dynamic picture of the above-mentioned three processes may require *in situ* real-time measurements, with different Au evaporation rates.

The metallic behavior of tunneling spectroscopy over Au clusters shows that a C₆₀ monolayer does not provide a tunneling barrier sufficient to form a single-electron-tunneling device,¹⁵ i.e., the barrier resistance is smaller than the quantum resistance $R_Q \equiv h/e^2$. This is due to the charge transfer from Au to C₆₀ monolayers. The situ-

ation will not be improved by a thicker film, due to the diffusion of Au atoms into additional C₆₀ layers.

CONCLUSIONS

This STM observation of Au overlayer formation on both the first and second C₆₀ monolayers on Au(111) substrate provides direct and detailed information about the Au-C₆₀ interface interaction, surface (or bulk) diffusion, and nucleation. At 300 K, Au forms clusters on top of the first C₆₀ monolayer, leaving the long-range close-packed structure undisturbed. Au atoms diffuse under the second C₆₀ monolayer and form 2D clusters. Such a cluster array provides multiple nucleation sites to rearrange the previously mobile second C₆₀ layer. As a result, the second layer becomes granulated. The bonding between C₆₀ grains and Au metal clusters, understood as a charge transfer from Au to C₆₀, is observed through the availability of states near the Fermi level. Our observation further confirms recent photoelectron spectroscopy results.³

ACKNOWLEDGMENTS

We wish to thank Sara Lutterbie for her help with the manuscript, and Myron Strongin for his support and encouragement. This work was supported by the U.S. Department of Energy under Contract No. DE-AC02-76CH00016 and Laboratory Directed Research Funds. It was also partially supported by the Air Force Office of Scientific Research, AFOSR Grant No. F49620-92-J-0358.

¹W. Kratschmer, L. D. Lamb, K. Fostiropoulos, and D. R. Huffman, *Nature* (London) **347**, 354 (1990); *Chem. Phys. Lett.* **170**, 1667 (1990).

²E. I. Altman and R. J. Colton, *Surf. Sci.* **279**, 49 (1992), and references therein.

³T. R. Ohno, Y. Chen, S. E. Harvey, G. H. Kroll, P. J. Benning, J. H. Weaver, L. P. F. Chibante, and R. E. Smalley, *Phys. Rev. B* **47**, 2389 (1993).

⁴S. H. Pan, S. Behler, M. Bernasconi, and H.-J. Güntherodt, *Bull. Am. Phys. Soc.* **37**, 167 (1992).

⁵J. W. Lyding, S. Skala, J. S. Hubacek, R. Brockenbrough, and G. Gamie, *Rev. Sci. Instrum.* **59**, 1897 (1988).

⁶J. A. DeRose, T. Thundat, L. A. Nagahara, and S. M. Lindsay, *Surf. Sci.* **256**, 102 (1991).

⁷K. Reichelt and H. O. Lutz, *J. Cryst. Growth* **10**, 103 (1971).

⁸J. E. Fischer, P. A. Heiney, A. R. McGhie, W. J. Romanow, A.

M. Denenstein, J. P. McCauley, Jr., and A. B. Smith III, *Science* **252**, 1288 (1991).

⁹S. Saito and A. Oshiyama, *Phys. Rev. Lett.* **66**, 2637 (1991).

¹⁰E. Burstein, S. C. Erwin, M. Y. Jiang, and R. P. Messmer, *Phys. Scr.* **T42**, 207 (1992).

¹¹J. M. Soler, A. M. Baro, N. Garcia, and H. Rohrer, *Phys. Rev. Lett.* **57**, 444 (1986).

¹²D. Sarkar and N. J. Halas, *Appl. Phys. Lett.* **63**, 2438 (1993).

¹³E. Ganz, K. Sattler, and J. Clarke, *Phys. Rev. Lett.* **60**, 1856 (1988).

¹⁴T. Chen, S. Howells, M. Gallagher, L. Yi, D. Sarid, D. L. Lichtenberger, K. W. Nebesney, and C. D. Ray, *J. Vac. Sci. Technol. B* **10**, 170 (1992).

¹⁵Z. Y. Rong, A. Chang, L. F. Cohen, and E. L. Wolf, *IEEE Trans. Magn.* **28**, 67 (1992); *Ultramicroscopy* **42-44**, 333 (1992).

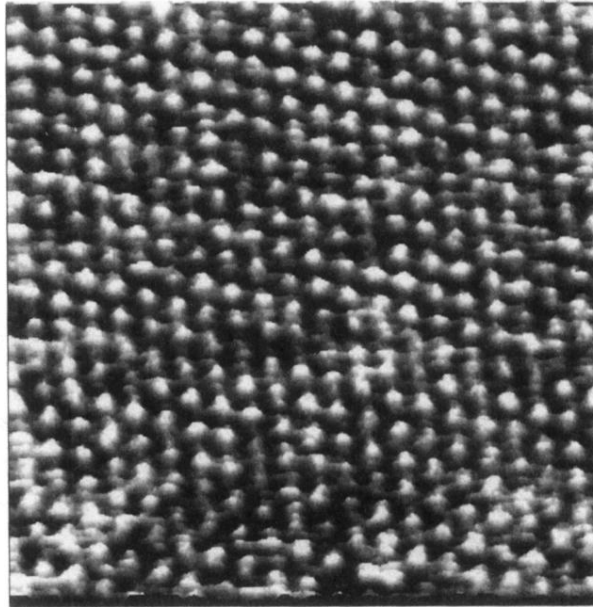


FIG. 2. Image ($61 \times 64 \text{ \AA}$) on a flat terrace of sample No. 1 (1000- \AA Au on mica). Tip bias voltage was +10 mV. The z corrugation is 0.13 \AA .

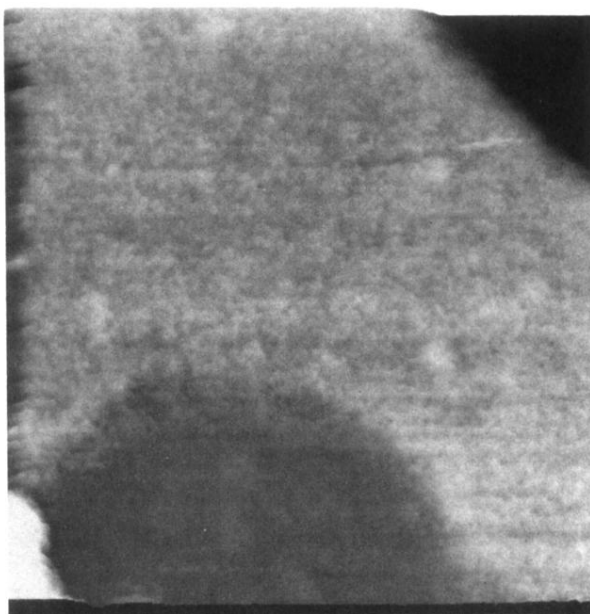


FIG. 3. Image ($1004 \times 1006 \text{ \AA}$) of C_{60} thin film of 1.7 ML on Au(111) (sample No. 2). Area inside the circular hole is identified as the first layer of C_{60} , while the outside is the second C_{60} monolayer. The layer spacing is 7 \AA .

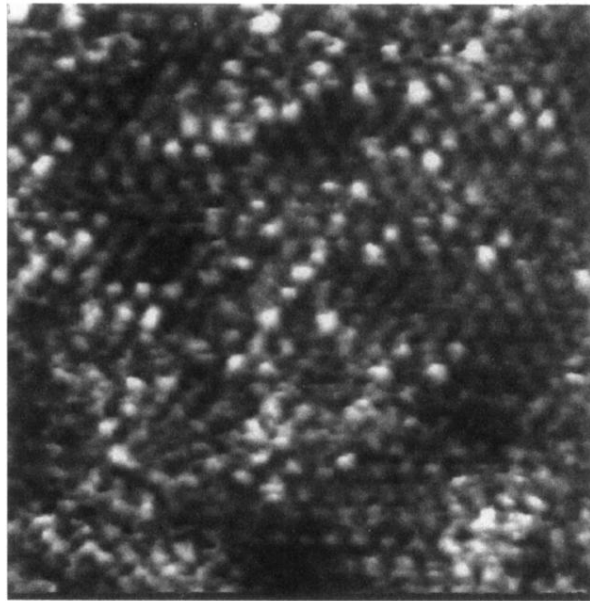


FIG. 4. Image ($230 \times 230 \text{ \AA}$) of the region inside the round hole in Fig. 3. The ordered close-packed lattice of C_{60} is shown. Periodicity is 11 \AA . Average corrugation is 0.8 \AA .

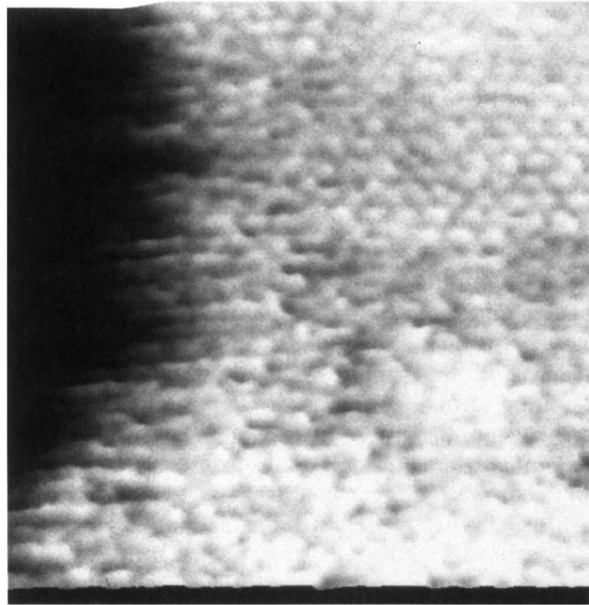


FIG. 5. Image ($214 \times 214 \text{ \AA}$) of the region at the right edge of the round hole in Fig. 3. The ordered close-packed structure is visible at the upper-right corner with a z corrugation of 2 \AA .

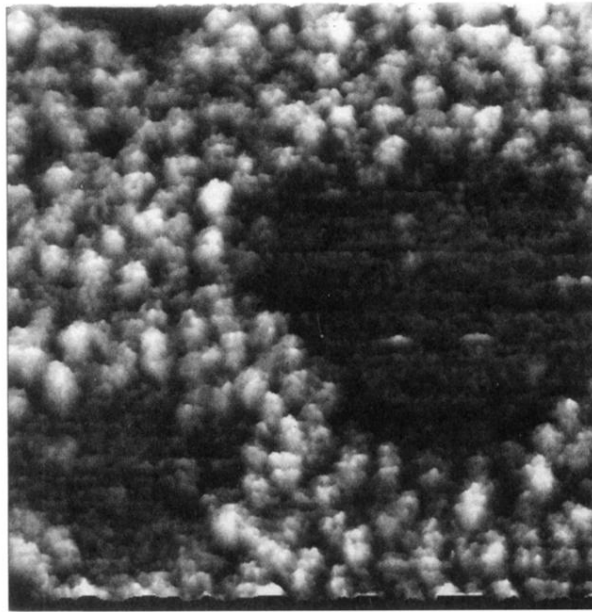


FIG. 6. Image ($1503 \times 1503 \text{ \AA}$) of sample No. 3 with 2 \AA of Au overlayers on top of a C_{60} thin film (similar to sample No. 2). It shows that a lower round region is flat and the higher region is granular. The granular region is 8 \AA higher than the flat region. The average z corrugation between grains is 3 \AA . The average grain-grain distance is 90 \AA .



FIG. 7. Image ($303 \times 303 \text{ \AA}$) inside the flat region in Fig. 6. The bright hill is around 80 \AA in diameter and 8 \AA in height. The underlying ordered structure is the same as in Fig. 4, with a z corrugation of about 0.8 \AA .

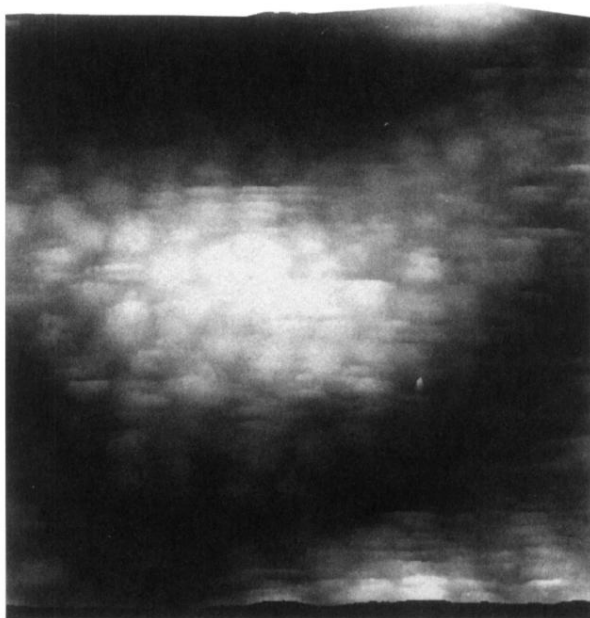


FIG. 8. Image ($152 \times 152 \text{ \AA}$) of a single grain on the higher region in Fig. 6. Images of the locally ordered C_{60} lattice are much easier to obtain than in Fig. 5. The average z corrugation is 0.8 \AA .